



2nd International Conference on Sustainable Energy Engineering and Application, ICSEEA 2014

Thermodynamic cycle evaluation of rhombic drive beta-configuration Stirling engine

Mohd Farid Zainudin^a, Rosli Abu Bakar^{a,*}, Gan Leong Ming^a,
Tanti Ali^a, Billy Anak Sup^a

^a*Faculty of Mechanical Engineering, Universiti Malaysia Pahang, 26600 Pekan, Pahang, Malaysia*

Abstract

The progressive developments and improvements of Stirling engines show significant effort in reducing the global emission level. The ability to use multiple kinds of heat sources with low emission level make it as a promising alternative solution in providing a healthier environment for natural population. For the present work, the thermodynamic cycle evaluation is conducted to a numerical model of proposed design of single-cylinder rhombic drive beta-configuration Stirling engine. The evaluation is carried out based on Schmidt ideal adiabatic model presented by Berchowitz and Urieli. The evaluation is based on three working space volumes of proposed beta-configuration engine. The prediction of reciprocating displacement, engine volumetric displacement, working fluid cycle pressure, working fluid instantaneous mass, cyclic energy flow and cyclic temperature are carried out and discussed. The proposed design's performance can be enhanced by maximizing the operating temperature difference between heat and sink source. Besides, the pressurization method could increase the thermal energy absorption and rejection thus enhancing the engine performance.

© 2015 The Authors. Published by Elsevier Ltd. This is an open access article under the CC BY-NC-ND license (<http://creativecommons.org/licenses/by-nc-nd/4.0/>).

Peer-review under responsibility of Scientific Committee of ICSEEA 2014

Keywords: thermodynamic cycle; rhombic drive; beta-configuration

1. Introduction

Nowadays, the continuous combustion of fossil fuels from fossil-based power generators caused not only negative impact to the environment and society, but also towards the increment of global emission level [1]. Due to

* Corresponding author. Tel.: +60 174 794 470.
E-mail address: mfz1421@gmail.com

this condition, the progressive developments and improvements of power generator technology show great efforts in providing a healthier environment for natural population. Stirling engine is one example of externally-heated power conversion device that uses external heat source to produced mechanical energy. The Stirling engine provides significant advantages whereby it can be easily designed and constructed due to exclusion of internal combustion process [2]. Besides, the high efficiency and ability to use multiple kinds of heat sources with low emissions level make the Stirling engine as a promising alternative solution in producing environmental-friendly energy conversion device [3]. Since the Stirling engine is externally-heated, the ability of using renewable energy sources such as solar, biomass, geothermal or even hybrid thermal energy system shows extensive usage of Stirling engine for energy conversion systems, for instance in parabolic Dish-Stirling system [4].

In the present work, the thermodynamic cycle evaluation is conducted to a numerical model of proposed design of single-cylinder rhombic drive beta –configuration Stirling engine. The prediction of reciprocating displacement, engine volumetric displacement, working fluid cycle pressure, working fluid instantaneous mass, cyclic energy flow and cyclic temperature are carried out and discussed.

2. Methodology

2.1. Numerical model

For the thermodynamic cycle evaluation of rhombic drive beta-configuration Stirling engine, a methodology presented by Berchowitz and Urieliis adopted. The evaluation is carried out by using an ideal adiabatic model based on Schmidt theory, which utilizes five volumes based on simplified engine model [3]. For the present work, a similar approach is applied to the working space volumes of the proposed design of beta-configuration Stirling engine. Fig 1 shows the schematic diagram of single-cylinder rhombic drive beta-configuration Stirling engine. The working space is divided into three spaces, which are the expansion space (hot-end), regenerator space, and compression space (cold-end). The expansion space volume varies over a cycle with the movement of the displacer piston. The regenerating space volume is based on the annulus between the displacer piston and displacer cylinder. The compression space varies due to the movement of both displacer and power piston. Meanwhile, the geometrical variables of the rhombic drive beta-configuration Stirling engine are listed in Table 1.

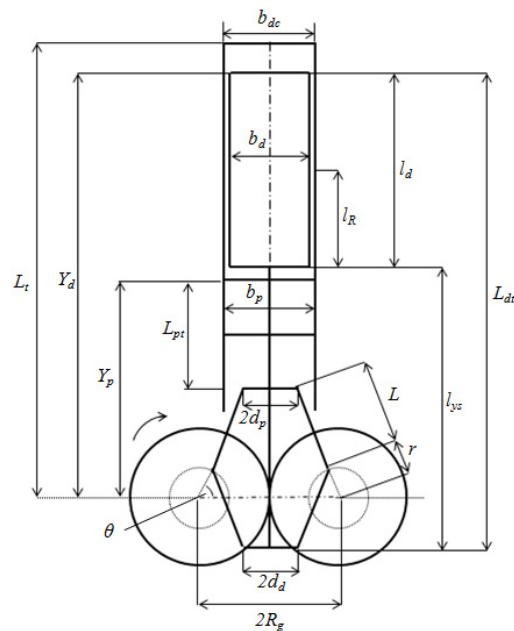


Fig 1. Schematic diagram of rhombic drive beta-configuration Stirling engine.

Table 1. Geometrical variables of the rhombic drive beta-configuration Stirling engine.

Components	Label	Dimension (mm)
Total length	L_t	416
Displacer cylinder bore	b_{dc}	84
Displacer piston length	l_d	182
Displacer piston bore	b_d	81
Regenerator length	l_R	152
Power piston length	L_{pt}	50
Power piston cylinder bore	b_p	80
Displacer piston yoke shaft	l_{ys}	262
Power piston yoke	$2d_p$	50
Displacer piston yoke	$2d_d$	50
Connecting rod length	$L_p=L_d=L$	80.5
Crank offset radius	r	38
Spur gear pitch diameter (PCD)	$2R_g$	130

2.2. Tables

Based on previous Fig. 1 and Table 1, the reciprocating displacements of the displacer and power piston connected with the rhombic drive mechanism, Y_d and Y_p are given as [5],

$$Y_d = L_{dt} + r \sin \theta - \left[L^2 - (R - d_p - r \cos \theta)^2 \right]^{1/2} \tag{1}$$

$$Y_p = L_{pt} + r \sin \theta + \left[L^2 - (R - d_p - r \cos \theta)^2 \right]^{1/2} \tag{2}$$

2.3. Volumetric displacements

The volumes of the expansion and compression space, V_E and V_C can be calculated, respectively in terms of Y_d and Y_p and the cross-sectional area of the cylinder. The expression of volumetric displacements for expansion and compression space can be further written as,

$$V_E = \pi b_d^2 \left\{ L_t - \left[L_{dt} + r \sin \theta - (L^2 - (R_g - d_d - r \cos \theta)^2)^{1/2} \right] \right\} \tag{3}$$

$$V_C = \pi b_p^2 \left\{ \left[L_{dt} + r \sin \theta - (L^2 - (R_g - d_d - r \cos \theta)^2)^{1/2} \right]^2 - \left[L_{pt} + r \sin \theta + (L^2 - (R_g - d_d - r \cos \theta)^2)^{1/2} \right]^2 - l_{ys} \right\} \tag{4}$$

2.4. Pressure

Using the ideal-gas equation of state, the working fluid pressure contained in the cylinder is calculated by following equation,

$$P = MR / \left(\frac{V_C}{T_C} + \frac{V_K}{T_K} + \frac{V_R}{T_R} + \frac{V_H}{T_H} + \frac{V_E}{T_E} \right) \tag{5}$$

where

$$T_R = \frac{T_H - T_K}{\ln(T_H/T_K)}$$

2.5. Working fluid instantaneous mass

The equations for mass in each component,

$$m_C = P \cdot V_{SWC} / (R \cdot T_C) \quad (6)$$

$$m_K = P \cdot V_K / (R \cdot T_K) \quad (7)$$

$$m_R = P \cdot V_R / (R \cdot T_R) \quad (8)$$

$$m_H = P \cdot V_H / (R \cdot T_H) \quad (9)$$

$$m_E = P \cdot V_{SWE} / (R \cdot T_E) \quad (10)$$

Therefore, the total mass of the working fluid remains constant,

$$m_C + m_K + m_R + m_H + m_E = M \quad (11)$$

2.6. Cyclic energy flow

Equations for energy in each space,

$$dQ_K = c_V \cdot V_K \cdot \frac{dP}{R} - (c_P \cdot T_{CK} \cdot m_{CK} - c_P \cdot T_{KR} \cdot m_{KR}) \quad (12)$$

$$dQ_R = c_V \cdot V_R \cdot \frac{dP}{R} - (c_P \cdot T_{KR} \cdot m_{KR} - c_P \cdot T_{RH} \cdot m_{RH}) \quad (13)$$

$$dQ_H = c_V \cdot V_H \cdot \frac{dP}{R} - (c_P \cdot T_{RH} \cdot m_{RH} - c_P \cdot T_{HE} \cdot m_{HE}) \quad (14)$$

$$W = W_E + W_C \quad (15)$$

$$dW = dW_E + dW_C \quad (16)$$

$$dW_E = P \cdot dV_E \quad (17)$$

$$dW_C = P \cdot dV_C \quad (18)$$

2.7. Cyclic temperature

The temperature changes in expansion, compression and regenerating space,

$$dT_E = T_E \cdot \left(\frac{dP}{P} + \frac{dV_{SWE}}{V_{SWE}} - \frac{dm_E}{m_E} \right) \quad (19)$$

$$dT_C = T_C \cdot \left(\frac{dP}{P} + \frac{dV_{SWC}}{V_{SWC}} - \frac{dm_C}{m_C} \right) \quad (20)$$

3. Results and discussions

Based on the engine geometrical variables, the reciprocating displacement for both displacer and the power piston is shown in Fig 2. During the engine cycle, the displacer moves at a 90 degree phase angle ahead of the power piston in order to draw the working fluid traversing back and forth between the expansion and compression space for heating and cooling process. At some instants, the displacer and the power piston were rather closed to each other, in the crank interval from 20 – 120-degree crank angle. During this condition, the minimum distance between the displacer lower and power piston top surface is treated to be influential factors that affect the dead volume of the engine. Less minimum distance means smaller dead volume in the compression space and more working fluid in the compression space being drawn into the expansion space for heating provided the power piston and the displacer do not coincide with each other [5].

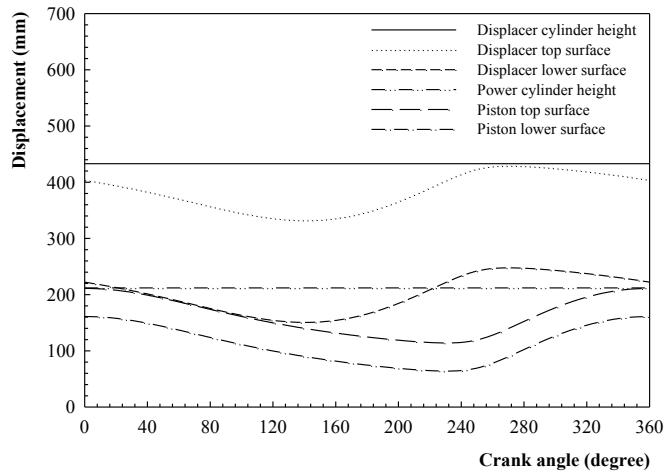


Fig 2. Reciprocating displacements.

Fig 3 shows the engine volumetric displacements based on rhombic drive mechanism. As the power piston and displacer are moving downwards, the volume in expansion space increased while the volume in the compression space remains in minimum since there is a minimum clearance between both displacer and piston. After a short while, the volume in the expansion space reaches its maximum and starts to decrease while the compression volume in the compression space is increased. At particular crank angle, when the volume of the expansion space reaches its minimum, the compression volume in the compression space reaches its maximum almost at the same time.

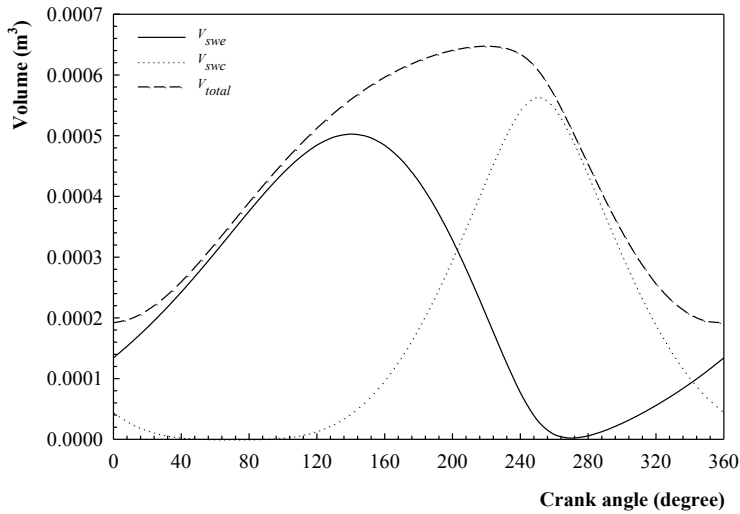


Fig 3. Engine volumetric displacements.

The working fluid cycle pressure is shown in Fig 4. Based on the expansion space’s temperature of 893 K and cold space’s temperature of 303 K, the pressure varies from 1.7 to 10.1 bars during the engine cycle. Based on the engine volumetric displacement shown in previous Fig 3, the working fluid pressure reaches its maximum as the engine total volume reaches its minimum. At particular crank angle position, the pressure is decreased as the both displacer and power piston moving downwards in which resulting an increment in expansion and total volume inside the engine. After certain period, the pressure starts to increase as the power piston moving upwards in which resulting the decrement of compression volume in the compression space. Meanwhile, the P-V diagram for proposed BCSE design is shown in Fig 5.

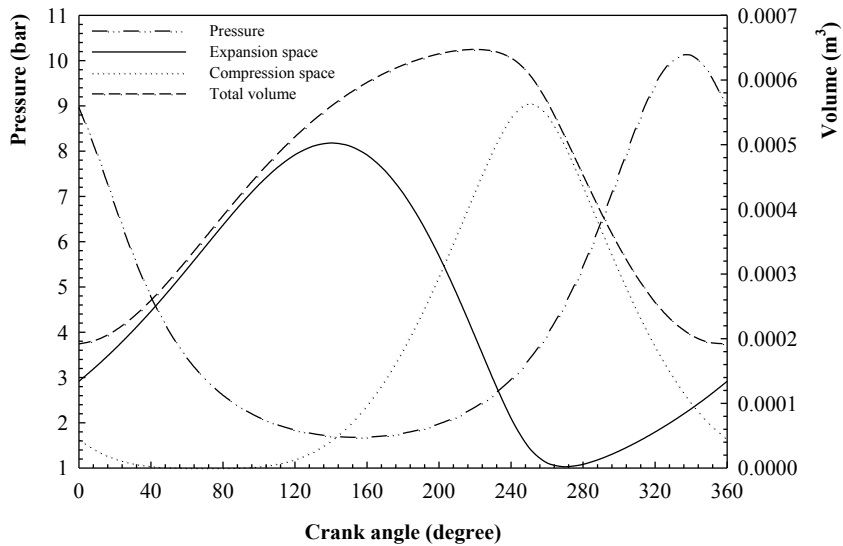


Fig 4. Engine cycle pressure.

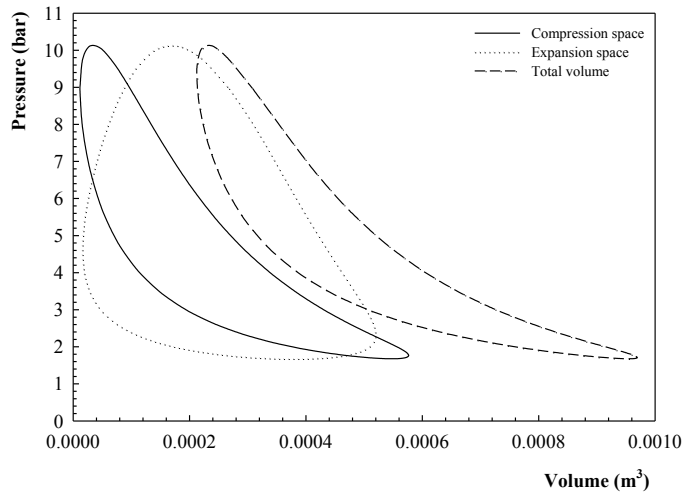


Fig 5. P-V diagram for beta-configuration Stirling engine.

Fig 6 shows the instantaneous mass of working fluid in each space. The pressure variation is also shown to indicate the interaction between mass and pressure within the heater, cooler, and regenerator spaces. The total amount of working fluid mass in the engine remains constant since there is an assumption that the engine has a perfect sealing so that there is no leakage of working fluid mass during engine operation. Based on this figure, the instantaneous mass of working fluid in the compression space is almost a direct mirror image of that of the expansion space. This indicates that most of the working fluid is within the compression space during heat rejection process. Similarly for expansion space, most of the working fluid is within the expansion space during the expansion process. Based on mass variation plot, higher thermal energy from the heat source can be absorbed by the working fluid since most of the mass is transferred to the expansion space. Higher thermal energy is rejected to the sink source since most of the working fluid mass is flows to the compression space [6].

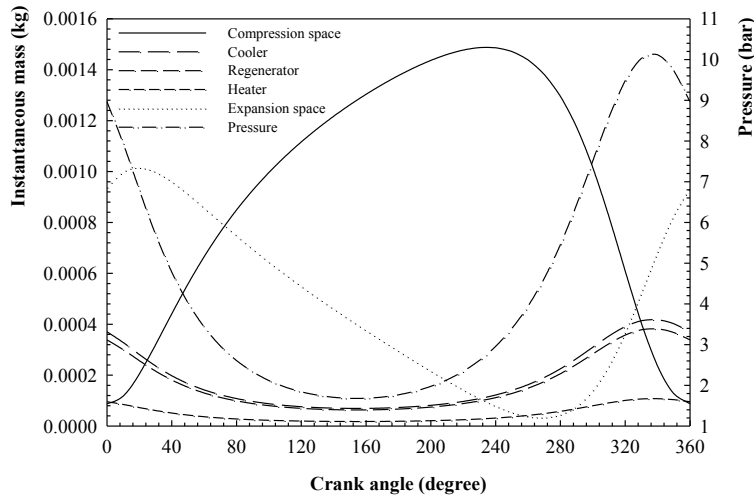


Fig 6. Working fluid instantaneous mass in each engine space.

Fig 7 shows the cyclic energy flow in the three heat exchangers of the engine as well as the total work done over a cycle. The result indicates that the energy flow in the regenerator is greater than that of the heater and cooler within the engine cycle. The energy flow in the regenerator is about two times larger than that of the heater and about 20 times larger than that of the cooler. In the other words, the heat transfer capacity of the heater and cooler is respectively 2 and 20 times less than that of the regenerator. As recommended by Reader (1983), the regenerator must be able to deal with larger heat load of the heater. However, if the regenerator is not been able to deal with larger heat load, the extra load will be placed on the other heat exchangers which reduces the internal operating temperature difference and thus reduces the engine power [7]. Meanwhile, the engine performance results can be found in the Table 2.

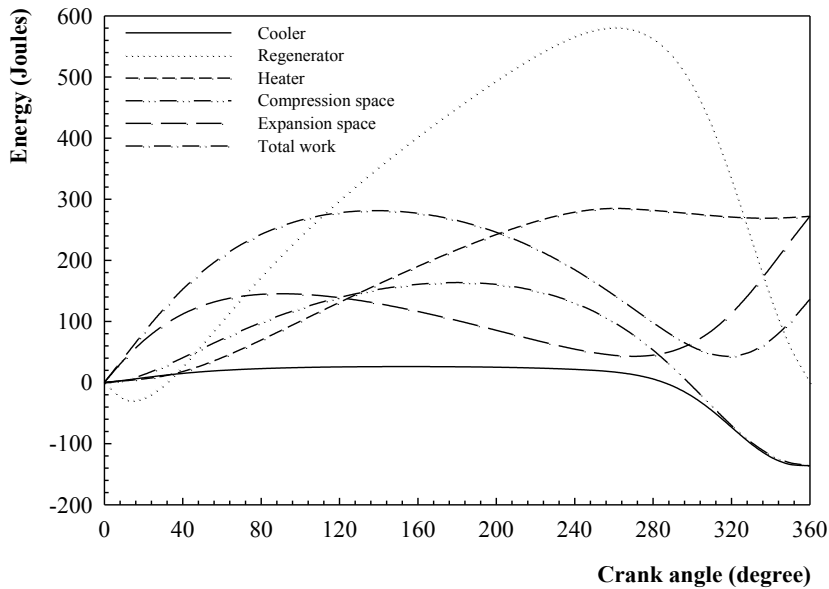


Fig 7. Cyclic energy flow in each engine space.

Fig 8 shows the cyclic temperature variation of the expansion and compression spaces as well as the heater, cooler, and regenerator temperature. Aligned with the assumptions of perfect heat exchangers and regenerator, the working fluid in heater and cooler is maintained at isothermal condition. However, the temperature within the expansion and compression space varies over the cycle in accordance with adiabatic nature of these working spaces [3]. The influence of the heater temperature during heating and the cooler temperature during the cooling process is clearly observed. The increases in expansion space temperature can be easily explained, at which the heat is added to the working fluid during the expansion process. Meanwhile, the decreases in compression space temperature are because of the heat in the working fluid is rejected to the cooler space during the compression process for energy conversion from heat into mechanical work [8].

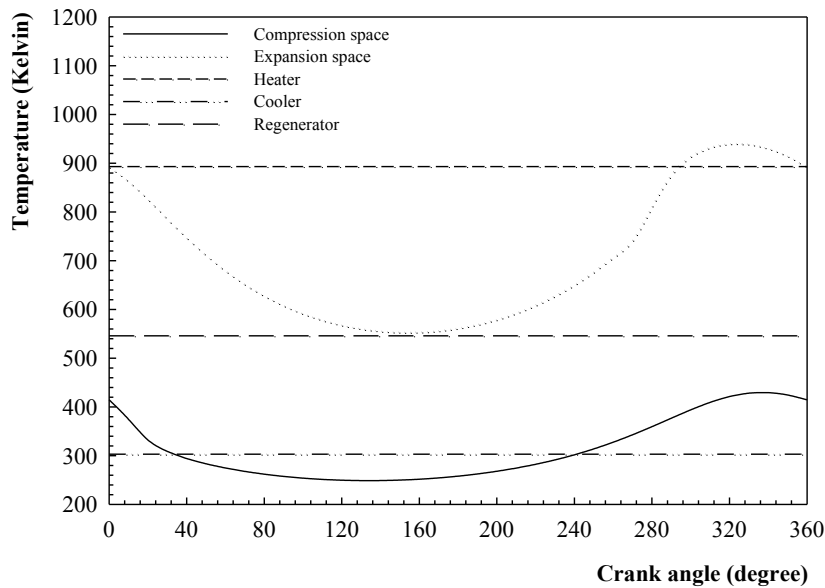


Fig 8. Cyclic temperature of the working fluid.

Table 2. Engine performance prediction results.

Parameters	Numeric value
Working fluid mean pressure (bar)	4.5
Working fluid mass (kg)	0.00128
Heat transferred to the heater (Watts)	1360.27
Heat transferred to the cooler (Watts)	-680.33
Thermodynamic cycle power (Watts)	805
Thermal efficiency (%)	50.1

4. Conclusions

The prediction of proposed design performance is carried out based on the numerical model for rhombic drive beta-configuration Stirling engine. The prediction of reciprocating displacement, engine volumetric displacement, working fluid cycle pressure, working fluid instantaneous mass, cyclic energy flow and cyclic temperature based on the proposed engine design are presented and briefly discussed. From the simulation results, the proposed design produced 805 W of power output at 300 rpm, based on designated operating temperature and typical engine operating speed that operates at atmospheric pressure. However, the engine's performance can be enhanced by maximizing the operating temperature difference between the heat source and sink source. Besides, the pressurization method is useful to enhance the thermal energy absorption and rejection during the engine cycle since there is an increase in working fluid mass.

Acknowledgements

The authors would like to thank the Fusion A&T Sdn. Bhd. for their financial support and thank to Universiti Malaysia Pahang for providing facilities for the development of engine working prototype.

References

- [1] Sripakagorn A, Srikam C. Design and performance of a moderate temperature difference Stirling engine. *Renewable Energy* 2011;36:1728-1733.
- [2] Kongtragool B, Wongwises S. A review of solar-powered Stirling engines and low temperature differential Stirling engines. *Renewable and Sustainable Energy Reviews* 2003;7:131-154.
- [3] Thombare DG, Verma SK. Technological development in the Stirling cycle engines. *Renewable and Sustainable Energy Reviews* 2008;12:1-38.
- [4] Abbas M, Boumeddane B, Said N, Chikouche A. Dish Stirling technology: A 100 MW solar power plant using hydrogen for Algeria. *International Journal of Hydrogen Energy* 2011;36:4305-4314.
- [5] Cheng CH, Yu YJ. Numerical model for predicting thermodynamic cycle and thermal efficiency for a beta-type Stirling engine with rhombic drive mechanism. *Renewable Energy* 2010;35:2590-2601.
- [6] Rogdakis ED, Antonakos GD, Koronaki IP. Thermodynamic analysis and experimental investigation of a solo V161 Stirling cogeneration unit. *Energy* 2012; 45:503-511.
- [7] Snyman H. Second order analyses methods for Stirling engine design. Master Thesis. University of Stellenbosch. 2007.
- [8] Tarawneh M, Al-Gathian F, Nawafleh MA, Al-Kloub N. Numerical simulation and performance evaluation of Stirling engine cycle. *Jordan Journal of Mechanical and Industrial Engineering* 2010;4:615-628.